ELSEVIER

Journal of Chromatography A, 922 (2001) 63–76

JOURNAL OF CHROMATOGRAPHY A

www.elsevier.com/locate/chroma

Macroporous copolymer matrix IV. Expanded bed adsorption application

Deba Prasad Nayak, Surendra Ponrathnam*, C.R. Rajan

Chemical Engineering Division, National Chemical Laboratory, Pune 411 008, India

Received 18 September 2000; received in revised form 6 April 2001; accepted 26 April 2001

Abstract

Macroporous crosslinked hydroxyethyl methacrylate–ethylene dimethacrylate copolymeric beads (HEG beads) were synthesized by suspension polymerization in the presence of a pore generating agent. These beads were coupled to α-cyclodextrin through a urethane spacer. These modified copolymer beads (affinity-HEG beads) so prepared were evaluated for their suitability in expanded bed chromatography. The optimum thickness of the distributor plate for stable expanded bed for use in expanded bed adsorption (EBA) was established. The affinity-HEG beads are comparable in density to Streamline diethyl amino ethane (DEAE) and exhibit better mechanical stability at higher superficial velocity under fluidization. The affinity-HEG beads were used as affinity chromatography matrices for the purification of cyclodextrin glycosyltransferase. Feeding of 5-fold diluted fermented broth to the column containing affinity-HEG beads of settled bed height 7.5 cm (I.D. 26 mm and length 42 cm) at double bed expansion resulted in a sharp breakthrough curve of α-cyclodextrin glycosyltransferase (CGTase). The adsorbed enzyme was eluted from the bed in 50 m*M* Tris–HCl buffer containing 10 m*M* $CaCl_2$ at 25°C in packed bed configuration.

Keywords: Macroporous copolymer beads; Affinity-HEG beads; Expanded bed adsorption; Affinity adsorbents; α-Cyclodextrin glycosyltransferase

1. Introduction

Expanded bed adsorption (EBA) chromatography is becoming increasingly popular due to its simplicity as a single step operation for purification of various proteins [1–4]. In this process, the feed is passed through the column from the bottom at an appropriate superficial velocity to expand the bed comprising dense polymeric adsorbent matrices. As a result, sufficient void spaces are created to allow submicron particles, including cells and undesired proteins, to pass through the column while the protein of interest is captured. The column is washed in expanded bed mode from bottom to top and the elution is carried out in packed bed mode in the reverse direction at lower velocity.

The success of this unit operation in protein purification is in part due to appropriate design regarding the distributor plate and the dense polymeric adsorbent [5]. The distributor plate distributes the feed liquid uniformly by imparting sufficient pressure drop by itself, whereas the particle size and density distributed adsorbents expand and segregate at differing parts of the bed at higher flow velocity to stabilize the bed. The matrices traditionally used for

*Corresponding author. Fax: +91-20-589-3041.

E-mail address: ponrathnam@che.ncl.res.in (S. Ponrathnam).

0021-9673/01/$ – see front matter
PII: S0021-9673(01)00923-2

expanded bed adsorption are crosslinked agarose-based quartz composite materials (Streamline, marketed by Amersham Pharmacia, Sweden), denser glass-coated agarose beads (marketed by Upfront Chromatography, Denmark) and silica composite chromatographic matrices (S-Hyper D LS, marketed by Biosepra, Marlborough, MA, USA). It is generally observed that after a large number of cycles Streamline composites tend to lose the heavy particles (quartz) at higher velocity on use with high viscosity fluids. Although there have been very many reports on studies with various composites for use in EBA, most have not been commercialized: cellulose/TiO_2 composite materials derivatized into diethyl amino ethane (DEAE) [6], fluoride modified zirconia supports [7] and crosslinked cellulose macroporous beaded adsorbents — cellbeads [8]. The composites of crosslinked cellulose and silica may have limitations due to chemical instability in acidic solution due to the acid-catalyzed hydrolysis of the siloxane bonds (Si–O–Si) anchoring the bonded phase to the surface [9]. The smaller size zirconia supports may block the distributor plate and support screen under fluidization operation. Asif et al. reported that medium density beads (1.6 g/ml) distort the bed hydrodynamics [10]. This suggests application of cellbeads and matrices of similar densities (commercialized by Upfront Chromatography) would create higher liquid dispersion in expanded beds.

The objective of this study is to evaluate the hydrodynamic characteristics of macroporous, crosslinked hydroxyethyl methacrylate–ethylene dimethacrylate (HEG) copolymer beads synthesized in our laboratory. These beads were modified by coupling with α-cyclodextrin. The affinity-HEG beads so prepared were used as affinity chromatography matrices for purification of α-cyclodextrin glycosyltransferase (CGTase) on EBA mode. The evaluation of the effect of adsorption of α-CGTase at various dilution rates is reported.

2. Experimental

2.1. Materials

The monomers 2-hydroxyethyl methacrylate (HEMA) and ethylene dimethacrylate (EGDM) used for the copolymerization were procured from Fluka, Germany. α-Cyclodextrin (CD) was a kind gift from Cerestar (USA). 2,4-Tolylene diisocyanate (TDI) used as spacer was obtained from Sigma–Aldrich (USA). The analytical grade 1,4-dioxane, dimethyl sulfoxide (DMSO), methylene chloride and methyl salicylate were procured from SD Fine Chemicals (Boisar, India). All media components were obtained from HiMedia (Mumbai, India). Soluble starch was from E-Merck (Mumbai, India). Streamline DEAE adsorbents were kindly given by Amersham Pharmacia (Uppsala, Sweden). Magnafloc was a kind gift from DuPont, USA.

2.2. Methods

2.2.1. Adsorbents

The beaded, macroporous copolymeric matrices were synthesized by suspension copolymerization of 2-hydroxy ethyl methacrylate (HEMA) and ethylene dimethacrylate (EGDM) in a jacketed cylindrical polymerization reactor [11]. These are abbreviated as HEG beads for simplicity. The matrices were coupled to α-CD using 2,4-tolylene diisocyanate (TDI) to yield affinity matrices for purification of α-CGTase. This is abbreviated as affinity-HEG beads [12]. α-CD bound on the matrices was assayed by the methyl orange method [13]. The affinity matrices were gradually added to a solution comprised of 2 ml methyl orange solution (18.32 μg/ml in water), 1.1 ml distilled water and 0.1 ml 1 N HCl until the decrease in absorbance was ~5–6%. The HEG beads were used as control in these assays.

The affinity-HEG and Streamline DEAE beads were wet sieved between diameter 105–355 and 105–250 μm (test sieves, Jayant Scientific, Mumbai, India), respectively. The bead diameters were determined by observation under microscope (Lietz, Germany) with a measuring device. The particle size was calculated from volume moment mean of 70–80 particles in five sets of observations. The standard deviation was less than 5% of the total diameter in all observations. The density of each size fraction of Streamline DEAE and affinity-HEG beads was measured under swollen state by flotation method [14]. The solvent mixture used in this experiment was methylene chloride and methyl salicylate.

2.2.2. Swelling of HEG beads

A 10-g amount of HEG beads was tested for swelling in water, 50 m*M* Tris–HCl buffer (pH 7.0, 8.0, 9.0 and 10.0), 1 N HCl and 1 N NaOH. The packed bed volume after swelling was noted. The skeletal volume of HEG beads was calculated by multiplying the packed bed volume by 0.6, considering the external void volume as 0.4. The skeletal volume of the dried HEG beads was calculated from the ratio of weight to density. The swelling ratio was calculated from the ratio of skeletal volumes in swelled and in the dry state.

2.2.3. Non-specific adsorption

A 1-g amount of affinity-HEG beads (2 μmol of α-CD/g of dried matrix) was equilibrated with 0.05 *M* Tris–HCl buffer of pH 7.0 in a 50-ml conical flask to check for non-specific ionic interaction. To each flask 10 ml of 0.1 mg/ml bovine serum albumin (BSA) (made in 50 m*M* Tris–HCl buffer, pH 7.0) was added and shaken well at 12°C, 200 rpm for 8 h. The HEG beads with BSA solution served as control. BSA solution was also shaken under similar conditions, as described above, to check for change in activity of the native protein under identical conditions. The matrices were decanted and washed with 0.05 *M* Tris–HCl buffer (pH 7.0) at 12°C. The adsorbed protein under these conditions was eluted with 5 ml of 6 *M* urea solution. The desorbed protein was estimated, as described by Lowry et al. [15].

Similarly, hydrophobic interaction was studied at room temperature with protein solution containing 1 *M* NaCl while maintaining other parameters the same as for non-specific ionic interactions. The matrices were washed with 1 *M* NaCl solution at 25°C and eluted with 0.05 *M* Tris–HCl buffer (pH 7.0) at 12°C.

2.2.4. CGTase production

α-CGTase (E.C. 2.4.1.19) was produced by fermentation using *Klebsiella pneumoniae pneumoniae,* NCIM 5121, in a 1-l magnetically driven top suspended fermenter (Gallenkamp, UK) [16]. The optimised fermentation media and conditions described earlier were used [17].

2.2.5. Feed characteristics

The viscosity of the feedstock was measured by Bohlin CVO 50 cone and plate rheometer (Bohlin Instrument, UK) in double gap geometry with I.D. 40 mm and O.D. 50 mm in steady shear stress mode. The temperature of the rheometer was controlled at 10°C (±0.1°C) by means of computer controlled constant water bath (Julabo, Sweden).

The density of the feedstock was calculated from the ratio of the weight to the volume of 250 ml of the diluted feedstock. A total of 10 ml of the fermented broth of various dilutions was centrifuged at 9600 *g* for 20–30 min, supernatant was discarded and the residue from the centrifuged mass was dried at 60°C in a vacuum oven until constant weight was obtained. Dry cell weight of the samples was calculated from the dry weight of the residue per ml of the sample. Protein concentration and enzyme activity were analysed by the method of Lowry et al. [15] and Lejuene et al. [13].

The feed was centrifuged at 9600 *g* at 4°C for 30 min (Remi, Mumbai, India) to check the % clarification of fermented broth. The fermented broth was also flocculated by addition of 5 ml/l of Magnafloc and was stirred overnight at 4°C. The flocculated feed was clarified by centrifugation at 2300 *g* for 20 min at 10°C. Microfiltration of the feed was performed with tubular module membrane (channel diameter 2 mm with 19 channels, surface area 0.19 m^2; Techsep, France).

2.2.6. Measurement of uptake rate of enzyme

Adsorption kinetics of α-CGTase (34.2 U/ml) on affinity-HEG beads (α-CD concentration 6.65 mg/g of the matrix) were carried out at 12°C with a variety of dilutions of unclarified fermented broth. The fermented broth was diluted 2-, 5-, 10- and 20-fold in 50 m*M* Tris–HCl buffer, pH 7.0, in 250-ml conical flask. In each of the experiments performed to study the adsorption kinetics, 50 ml of diluted unclarified fermented broth was treated with 1 ml of affinity-HEG beads. These flasks were stirred at 100 rpm in controlled environment incubator shaker at 12°C (Psychrotherm™, New Brunswick Scientific, USA). A total of 0.5 ml of liquid was withdrawn from the flasks at 60-min intervals, centrifuged at 9600 *g* and assayed for α-CGTase. The decrease in volume of the liquid during experiment was less than 8%.

2.2.7. Expanded bed adsorption experiments

2.2.7.1. Stable bed characteristics with various distributor plates

The experimental set-up consisted of a jacketed column (I.D. 26 mm and length 42 cm having movable adapters) connected through a double jacketed glass vessel (600-ml volume), three-way valve and a six roller peristaltic pump (LKB, USA) to the bottom of the chromatographic column. The upper and lower adapter of the column of 26-mm diameter and 42-cm length (XK26, Pharmacia Biotech, Sweden) were modified to suit the higher flow-rate operated in the column.

Circulating cold water using constant temperature water bath (Julabo, Sweden) controlled the temperature of the whole system (at 10°C). The degree of expansion of affinity-HEG beads was measured at various flow velocities using various distributor plates. The distributor plates comprised of stainless steel (SS) plate of 1- and 2-mm thickness and tapered Deldrin plate of 2-mm thickness (15° angle). In each of the experiments with varying distributor plate, a support screen was incorporated facing towards the adsorbents. The expanded bed height was measured when the motion of the particles appeared visually to be stable. The initial bed height in all experiments was kept at 7.5 cm (bed volume 39.8 ml). The bed was equilibrated with 50 m*M* Tris–HCl buffer, pH 7.0, from one vessel and acetone (0.25%, v/v in same buffer) was used as tracer (step input) from other vessel by switching the three-way valve. The positive step input UV signal recorded until measurement of the maximum absorbance (100%) is called *F*-curve. The output signal was measured at 266 nm through a flow cell connected to a spectrophotometer (ATI Unicam UV/Vis spectrophotometer UV2, UK). When the signal at 266 nm stabilized, the buffer feeding was started from the flask-containing buffer by switching the three-way valve. Data were compiled with a personal computer.

The bed expansion was evaluated by the Richardson–Zaki equation $u = u_t \epsilon^n$ [18], where u is liquid superficial velocity, u_t the apparent terminal velocity, ϵ the bed voidage and n is the Richardson–Zaki coefficient. The value of ϵ was calculated from $H/H_0 = (1 - \epsilon_0)/(1 - \epsilon)$, where H_0 is the sedimented bed height, H is the expanded bed height and ϵ_0 is the voidage in the sedimented bed. In this study a value of 0.4 was used for ϵ_0, as determined earlier [19,20]. Number of theoretical plates (N) was calculated as $N = t^2/\sigma^2$, where t is the residence time and σ^2 is the variance. The parameters t and σ were determined by residence time distribution (RTD) analysis for expanded bed mode from the *F*-curve using the procedure described by Levenspiel [21]. Mixing in the liquid phase was evaluated by determining axial dispersion. The axial dispersion coefficient D_{ax}, was calculated using $D_{ax} = uH/2N\epsilon$ [22], where u is the liquid superficial velocity, H is the bed height under expansion and ϵ is the bed voidage.

2.2.7.2. Frontal bed analysis of Streamline DEAE and affinity-HEG beads in expanded bed

Frontal bed analysis was carried out to compare the binding of α-CGTase on HEG beads. Various distributor plates (with 1-mm hole) were designed to compare the stability and adsorption characteristics in expanded bed. HEG beads were added to the column in separate experiments designed to study the effect of varying the distributor plates. The settled bed height was noted as 7.5 cm and the calculated bed volume was 39.8 ml. The bed was expanded to double the settled bed height and the flow of buffer (50 m*M* Tris–HCl buffer, pH 7.0) was continued for 45 min to 1 h to obtain a stable expanded bed at a flow-rate (19.8 ml/min) corresponding to 224 cm/h. Unclarified fermented broth of varying of dilutions (1, 2, 5, 10 and 20) was pumped into the bed at appropriate flow-rates (depending on the feed characteristics) to expand the bed to double its settled height. Fractions were collected at regular time intervals and assayed for α-CGTase, protein and cell mass. The bed was washed with 50 m*M* Tris–HCl, pH 7.0, and 10 m*M* $CaCl_2$ (prepared in 50 m*M* Tris–HCl, pH 7.0) consecutively at 10°C. The flow-rate was increased slowly to 19.8 ml/min to keep the bed under constant expansion. The washing was continued until that the outlet absorbance at 280 nm reached zero. The bed was allowed to settle by stopping the pumping of the washing buffer and the upper adapter was lowered down to pack the bed. The enzyme was eluted with 10 m*M* $CaCl_2$ in 50 m*M* Tris–HCl buffer, pH 7.0, at 25°C at a flow-rate

of 4.4 ml/min (50 cm/h). The bed was regenerated at 70°C with 2 *M* NaCl solution and washed with water in packed bed mode at a flow-rate of 4.4 ml/min.

3. Results and discussions

3.1. Adsorbent preparation and characteristics

3.1.1. Adsorbent preparation

The HEG beads, with a crosslink density of 25 mol.%, were synthesized by suspension polymerization in jacketed cylindrical polymerization reactor. Crosslink density (CLD) is defined as the mole percent of crosslinking divinyl monomer (ethylene dimethacrylate) (EGDM) relative to the moles of reactive functional vinyl comonomer (2-hydroxyethyl methacrylate) (HEMA). The continuous phase comprised of 250 ml of aqueous solution of 1% poly(vinyl pyrrolidone) (PVP). The discontinuous organic phase consisted of 21.6 ml of HEMA and 8.4 ml of EGDM. Cyclohexanol was used as inert component to control the porosity of the inner structure of the polymeric beads. The copolymerization was initiated by azo-bis-isobutyronitrile (AIBN) and carried out in 300-ml reactor, provided with six blade Ruston turbine impeller with controlled variable revolutions for 3 h at 70°C. After being cooled, the reaction product was repeatedly decanted with water and methanol, and dried at 60°C under vacuum.

The affinity-HEG beads were prepared by coupling the pending –OH group of HEG beads to –OH group of α-CD by urethane linkage through TDI. The activation step was carried out with 1:1 molar quantities of –CNO group (present in diisocyanate) with respect to –OH group in the HEG beads. This step was carried out in a conical flask with suitable aprotic solvent under stirring at 200 rpm for 24 h and dried N_2 environment. After completion of the activation step, the matrices were washed with anhydrous 1,4-dioxane. The second step was the coupling of the ligand (CD) to the activated matrices. α-CD solution was made in anhydrous DMSO and added to the activated matrices. The reaction was carried out under stirring at 200 rpm in 250-ml conical flask for 24 h.

3.1.2. Mechanical, microbial, chemical stability and non-specific interaction of affinity-HEG beads

The particle size distribution and the average density of the matrices are presented in Table 1. The standard deviation of five sets of experiments is within 6%. Owing to high crosslink density and low affinity for the aqueous environment, HEG beads exhibit low swelling (9.96 ml of dried HEG beads swell to 24.6 ml in 50 m*M* Tris–HCl buffer, pH 7.0). The swelling characteristics did not change with pH (1–12) and salt concentration 10 m*M* to 1 *M* of NaCl. The mechanical stability of the affinity-HEG beads was compared with Streamline DEAE by fluidizing for a week under stable expansion at a superficial velocity of 428 cm/h. The particle size distributions were evaluated at swollen state before fluidization and after fluidization under above-mentioned conditions. Comparative results between these two adsorbents presented in Table 2 point out that HEG beads are mechanically stable under fluidization condition at higher superficial velocity. During fluidization, 12.9% of the Streamline DEAE adsorbents were lost, while only 0.4% of affinity-HEG beads were similarly carried away. The instability of the Streamline DEAE at higher superficial velocity is

Table 1
Comparison of particle size and density distribution of affinity-HEG beads and Streamline DEAE

Particle size (μm)	HEG beads		Streamline DEAE	
	wt.% Of matrix	Density (g/ml)	wt.% Of matrix	Density (g/ml)
250–355	48.5	1.21	Nil	Nil
180–250	25.8	1.208	41	1.19
150–180	17.3	1.202	28	1.17
105–150	8.4	1.18	19	1.16
0–105	Nil	Nil	12	1.15

Table 2
Comparison of mechanical stability of affinity-HEG beads with Streamline DEAE

Particle size (μm)	Before fluidization				After fluidization			
	HEG beads		Streamline DEAE		HEG beads		Streamline DEAE	
	wt.% Of matrix	Density (g/ml)	wt.% Of matrix	Density (g/ml)	wt.% Of matrix	Density (g/ml)	wt.% Of matrix	Density (g/ml)
250–355	48.5	1.210	Nil	Nil	48.4	1.210	Nil	Nil
180–250	25.8	1.208	41	1.190	25.7	1.208	40.5	1.190
150–180	17.3	1.202	28	1.170	17.2	1.202	25.5	1.170
105–150	8.4	1.180	19	1.160	8.3	1.180	17.6	1.160
0–105	Nil	Nil	12	1.150	Nil	Nil	8.5	1.150

The beds were fluidized continuously for a week at superficial velocity 428 cm/h. The difference in particle size distribution before and after fluidization is the loss of particles from the bed.

due to leaking of quartz particles from the beaded adsorbents, which could be observed visually.

Our investigation of shaking 10 ml of 0.1 mg/ml BSA with 1 g of HEG beads in a shaker at 200 rpm at 12°C indicated the absence of non-specific ionic interactions, but negligible (90 μg BSA/g of dry matrix) hydrophobic interactions. HEG beads are also resistant to microbial attack. Exposure to air in moist condition is a test for microbial attack. The microbes in air may degrade the matrix if it could be attacked and this would reduce the size and flow characteristics. Therefore, the water-swollen beads were exposed to air for a month and the size and density distribution of the beads were evaluated and compared. There was no change in size and density distribution of the water-swollen affinity-HEG beads after exposure to air. Exposure of the HEG beads to 1 *M* NaOH, 1 *M* HCl and at elevated temperature (121°C) for 30 min did not change the size and density distribution of the particles. These findings indicate that the HEG beads are resistant to microbial, chemical and physical environments encountered in expanded chromatographic operation.

3.2. Effectiveness of flow distribution

To check the bed stability, various distributor plates were fabricated and tested in this study. The residence time distribution (RTD) test is a tracer stimulus method used to assess the degree of longitudinal axial mixing (dispersion) in the expanded bed by defining the number of theoretical plates (*N*). The matrices used in this study were affinity-HEG beads (average particle size, 258 μm; average particle density, 1.21 g/ml) and Streamline DEAE (average particle size, 198 μm; average particle density, 1.18 g/ml) in swollen state. The particle size and density distribution of affinity-HEG beads and Streamline DEAE are summarized in Table 1. Both beads have Gaussian type particle size distribution (Fig. 1). The hydrodynamic characteristics of Streamline DEAE and HEG beads were compared. The effectiveness of distributor plates of various thicknesses, with the metallic (SS) screen mounted on the side of the distributor plate facing the adsorbent, was investigated (Figs. 2 and 3) using affinity-HEG beads. The use of thin metallic support screen (12-mesh/cm^2) devoid of distributor plate results in lower distribution of the liquid in the bed. This was evident from lower number of theoretical plates (*N*) observed under these conditions. Therefore, 1- and 2-mm thickness distributor plates were fabricated. At lower

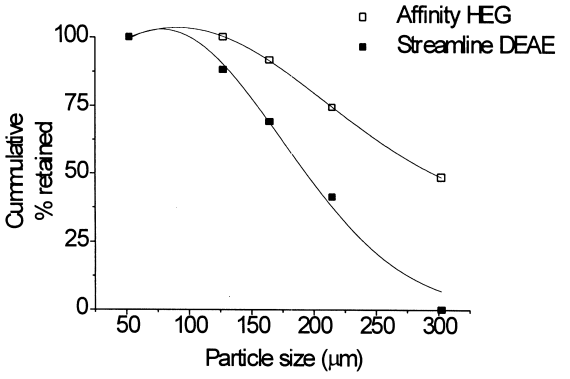

Fig. 1. Particle size distribution of Streamline DEAE and affinity-HEG beads.

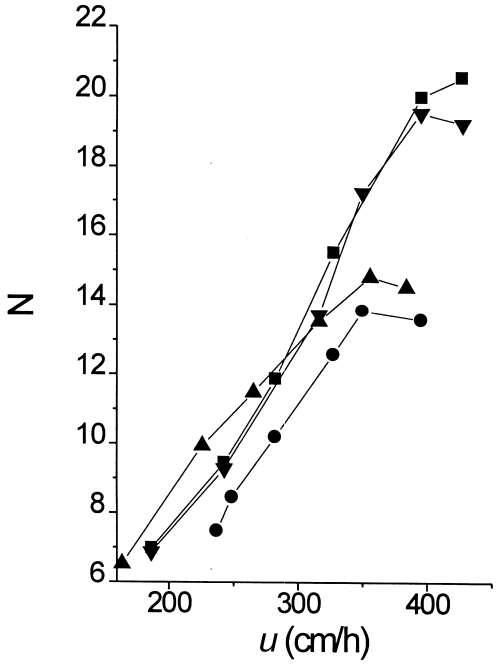

Fig. 2. Number of theoretical plates with varying superficial velocity of affinity-HEG beads. ● No distributor plate, ▲ perforated SS plate (1 mm), ▼ perforated SS plate (2 mm), ■ perforated tapered plate (2 mm).

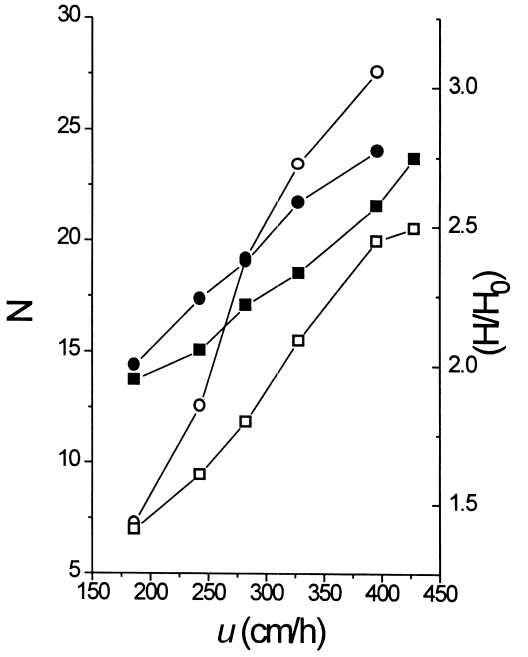

Fig. 3. Comparison of degree of expansion and number of theoretical plates of Streamline DEAE and affinity-HEG beads. ● H/H_0-Streamline DEAE, ■ H/H_0-affinity-HEG beads, ○ N-Streamline DEAE, □ N-affinity-HEG beads.

superficial velocity, the effect of liquid distribution depends upon the density of the holes [10]. It was suggested that maximum hole density of distributor plate be used for fluidized immobilization column. We have calculated the density of holes on the basis of packed bed porosity. It is assumed that the flow of the liquid passing through the distributor plate is comparable to the flow through the void spaces of a packed bed. Therefore, the ratio of hole cross-section area to distributor plate cross-section area was similar to the packed bed void space through which the liquid passes. The combined effect of perforated SS plate of 1-mm thickness (diameter of the hole, $D_{or}=0.1$ cm, hole density 20.73 holes/cm^2) and the support screen imparted more pressure drop and distributed the feed liquid throughout the bed. The number of theoretical plates of the bed containing 1-mm perforated SS plate and the support screen increased with superficial velocity with respect to the support screen. Thickness of the distributor plate has positive effect on the stability of the bed, which was evident from the increase in N. However, the additional effect due to the tapered configuration of the distributor plate (15° angle) was not observed from the number of distributor plates measured (Fig. 2), which is a measure of liquid dispersion in the bed. The pressure drop was also increased by increasing the thickness of the plate and keeping the diameter and the density of the holes constant. This helped in uniformly distributing the liquid in the bed. The degree of expansion of both the matrices with increase in superficial velocity (u) are shown in Fig. 2. The N versus u profile was found to increase for Streamline DEAE whereas with affinity-HEG beads N increased initially and then leveled off with increasing superficial velocity (Fig. 3). As is evident from Table 1, the density of affinity-HEG beads varies with bead size. Therefore, the gradation of affinity-HEG beads in the expanded bed is due to density and as well as the size of the beads. The axial dispersion coefficient (D_{ax}), which is a measure of liquid mixing in the bed, was measured for both the matrices using the tapered distributor plate under various flow-rates. At lower flow-rates, the disper-

Table 3
Bed expansion characteristics of affinity-HEG beads and Streamline DEAE at various flow velocities

u (cm/h)	HEG beads					Streamline DEAE				
	H (cm)	N	σ^2	$(D_{ax})\times10^6$ (m^2/s)	N/H_0 (m)	H (cm)	N	σ^2	$(D_{ax})\times10^6$ (m^2)	N/H_0 (m)
187	14.6	7.0	0.143	7.83	93	15.0	7.25	0.138	7.68	97
243	15.4	9.5	0.106	7.73	127	16.8	12.56	0.08	6.16	167
283	16.6	11.9	0.084	7.52	159	17.8	19.20	0.052	4.88	256
328	17.5	15.5	0.064	6.92	207	19.4	23.45	0.043	4.90	313
396	19.3	20.0	0.050	6.92	267	20.8	27.56	0.036	5.30	367
428	20.6	20.5	0.049	7.64	273	ND	ND	ND	ND	ND

In all the experiments, the settled bed height (H_0) was kept at 7.5 cm. N is the number of theoretical plates, σ^2 is the dimensionless variance and D_{ax} is the axial dispersion coefficient.

sion in both beds was similar. The dispersion in affinity-HEG bead increased and exceeded that of Streamline DEAE, with increase in degree of expansion (Table 3). The number of stages per settled bed height (N/H_0) is a measure of liquid dispersion. The value of N/H_0 was in the range of 93–273 and 97–367 for affinity-HEG beads and Streamline DEAE, respectively. This value is supported by Lindgren et al., who showed hydrodynamic properties of commercial material (Streamline), i.e. ~200 stages/m (N/H_0) [23]. The Richardson–Zaki coefficient for affinity-HEG beads was higher (6.62) than that for the Streamline DEAE beads (6.53). This indicates that at the same degree of expansion higher superficial velocity is observed for affinity-HEG beads than for the Streamline DEAE. The calculated terminal velocity was also higher for affinity-HEG (37.95 cm/min) beads than the Streamline DEAE matrices (31.55 cm/min). Karau et al. investigated the expanded bed characteristics of particles of varying diameter [24]. The authors observed experimental terminal settling velocities (U_t) ranging from 22.1 to 40.7 cm/min and Richardson–Zaki coefficients (n) between 4.9 and 5.5, respectively. Similarly, the values of n and U_t reported in buffer for particles of size 247 μm were 4.79 and 25.44 cm/min, respectively [25].

3.3. Feed characteristics

α-CGTase was produced by fermentation of *K. pneumoniae pneumoniae* in a 1-l fermenter at 600 rpm, in a fed-batch mode. The batch run was started with 0.5 l medium containing (in g/l) dextrin 49, urea 5, yeast extract 5, $(NH_4)H_2PO_4$ 6, $MgSO_4$ 0.2 and pH 7.0. After 6.5 h of batch cultivation, feed containing dextrin (172.5 g/l) and other components (at double the concentration used in batch mode of operation) was started. The feed rate was controlled using a feed-back control based on dissolved oxygen (DO), which was maintained between 0 and 25% of its saturation value. The addition of feed was complete after 15 h. The dry cell mass concentration, protein concentration, enzyme activity, density and viscosity of the fermented broth are listed in Table 4.

Table 4
Physical characteristics of the feed

Dilution factor	Dry cell wt. (g/l)	Protein (mg/l)	Enzyme activity (U/ml)	Density (g/l)	Viscosity (mPa s)	Shear rate (s^{-1})
1	65.20	13.42	34.20	1.023	98.20	0.075
2	32.40	6.74	17.12	1.015	42.04	0.476
5	13.80	2.65	6.81	1.013	21.67	0.923
10	6.42	1.32	3.40	1.010	21.59	0.926
20	3.20	0.65	1.70	1.005	21.05	0.950

The feed was diluted with addition of 50 m*M* Tris–HCl buffer, pH 9.0.

Centrifugation of the fermented broth at high speed (9600 *g*) resulted in 99% clarification. The partially clarified feed blocked the packed bed affinity starch column while loading. Therefore, the other alternative methods of clarification (flocculation and microfiltration) were performed. It was also observed that flocculation of the fermented broth by using flocculating agent (Magnafloc, 5 ml/l of fermented broth) and clarification by centrifugation at 2300 *g* for 20 min at 10°C resulted in more than 99.9% clarification without any loss in enzyme activity. The ionic flocculating agents may block the pores of ultrafiltration (UF) membranes and the resins used for concentration and clarification. Moreover, microfiltration (channel diameter 2 mm with 19 channels, surface area 0.19 m^2; Techsep, France) of the fermented broth gradually decreased the flux with time (reduced from 70 to 26 ml/min), thereby resulting in a longer filtration time (1 h 38 min for a volume of 3.38 l). A small fraction of the enzyme and protein were lost. By washing the retentate side of the membrane module with 50 m*M* Tris–HCl buffer (pH 7.0), 3.7% was recovered. The rest of the enzyme and proteins were found to be concentrated on the retentate side. Total recovery of the enzyme was 72% after washing. This resulted in a dilution of the clarified fermented broth to nearly double its initial volume. Furthermore, this enzyme is not stable for a long period of time in both unclarified and clarified fermented broths. These findings prompted us to select the fermented broth of α-CGTase as a model system for purification using EBA mode.

The feed characteristics comprised the properties dry cell weight, protein concentration, enzyme activity and density. DNase was reported to drastically lower the viscosity of the crude feedstocks [26]. However, the feed characteristics were varied with dilution, without the help of DNase addition. The values of these parameters decreased on dilution of the fermented broth. Viscosity of the diluted fermentation broth was found to decrease with dilution up to 5-fold and then to level off (Table 4). The exact reason for this anomalous behaviour of viscosity upon dilution is not known. However, *K. pneumoniae* produces extracellular polysaccharide bio-flocculent, which might participate in vivo bacterial aggregation [27]. The cell aggregation of *K. pneumoniae pneumoniae* may not decrease beyond 5-fold dilution of the fermented broth with the buffer, which is responsible for higher viscosity.

3.4. Measurement of uptake rate of enzyme

The effect of adsorption rate of the various diluted fermentation broths on the affinity-HEG beads was measured from the uptake rate of α-CGTase in a batch adsorption system (Fig. 4). The viscosity of the broth decreased with increasing dilution until 5-fold dilution and then remained unchanged until 20-fold dilution (Table 4). Therefore, the intraparticle diffusion rates in case of 5-, 10- and 20-fold dilution are similar. The other parameter, which affects the rate, is adsorption dissociation constant. Our previous study on batch adsorption of the clarified fermented broth had indicated that the adsorption pattern followed Langmuir isotherm [28]. The maximum adsorption capacity (Q_m) was 666 U/g of the adsorbent (containing 6.65 mg of ligand/g of adsorbent) and the dissociation constant was 6.21 U/ml [28]. Fig. 5 shows that the intraparticle diffusion was dominant up to double the dilution and that the rate of adsorption was slow. On the other

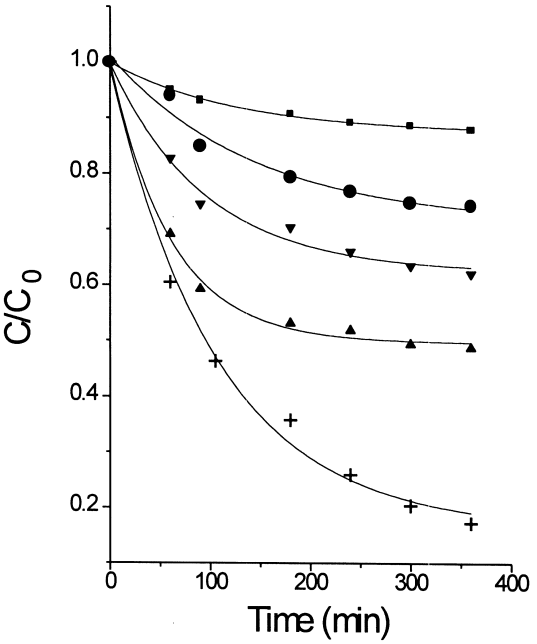

Fig. 4. Uptake curve for adsorption of α-CGTase on affinity-HEG beads at different dilutions of the fermented broth. ■ Undiluted, ● 2-fold diluted, + 5-fold diluted, ▲ 10-fold diluted, ▼ 20-fold diluted fermented broth.

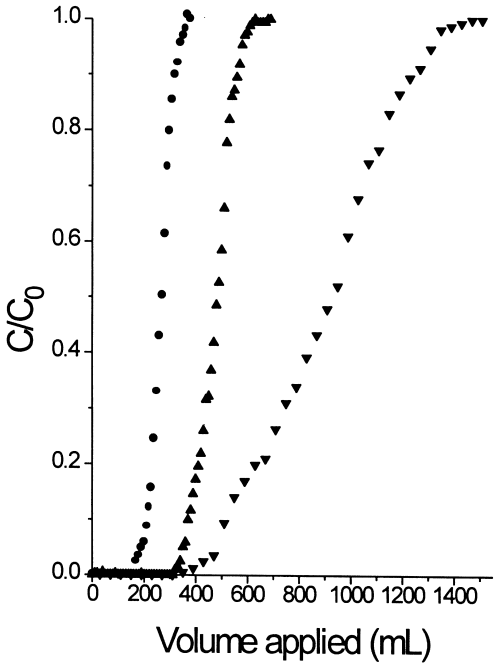

Fig. 5. Breakthrough curve of α-CGTase on affinity-HEG beads at different dilutions of the fermented broth. ● 5-fold diluted-105 cm/h, ▲ 10-fold diluted-130 cm/h, ▼ 20-fold diluted-152 cm/h.

hand, a comparison of 5-, 10- and 20-fold diluted feed samples shows the dominance of adsorption kinetics. Uptake rate of α-CGTase present in 5-fold diluted feed was faster than that from 10- and 20-fold diluted feed.

3.5. Frontal analysis in expanded bed

Similarities in the axial dispersion and breakthrough profile have been reported to be independent of the viscosity, density and superficial velocity of the feed at double expansion of the bed [25]. Therefore, the bed was expanded to double its settled bed height in all experiments (settled bed volume 39.8 ml, settled bed height 7.5 cm). In this expanded bed operation, the sample was fed continuously into the column until the available capacity of the column was exhausted and adsorbate began to appear on the column outlet. The variation of the concentration of the adsorbate in the column outlet as a function of time is known as breakthrough curve, and the measurement of breakthrough curves for such system is referred to as frontal analysis. The frontal analysis was employed to determine the dynamic adsorption capacity (*DAC*), dynamic adsorption rate (*DAR*), breakthrough volume (V_b) and breakthrough time (t_b) as well as the shape of the breakthrough curve. The flow velocities at which the feed of different dilutions expanded the bed to double the initial value were investigated. The flow of the feedstock at pH 9.0 to the affinity-HEG beads was continued until the enzyme activity of α-CGTase in the effluent equaled that in the feed CGTase. The bed dynamic adsorption capacity (*DAC*) was calculated by integrating the curve (volume applied versus effluent α-CGTase concentration) when enzyme activity in the effluent reached 5% of that in the feed. The efficiency of separation of α-CGTase was evaluated by calculating dynamic adsorption rate (*DAR*), defined as the ratio of *DAC* and breakthrough time:

$$q^* = \int_{v=0}^{v_{rf}} \frac{(C_0 - C)\,\partial V}{V_f} \quad (1)$$

where C_0 is initial concentration of adsorbate (U/ml), C is enzyme concentration in the effluent at time t (U/ml), V is volume of the feed applied to the column (ml), V_f is volume of the fluidized or the expanded bed (ml), v_{rf} is total volume passed through the bed (ml), and q^* is units of adsorbate bound to the adsorbent at equilibrium (U/ml).

The amount of enzyme applied to the column is given by:

$$m = C_0 \times t \times Q = C_0 \times v_{rf}$$

where Q is the volumetric flow-rate (ml/min).

In the graphical integration method, the area behind the curve also includes contributions from the dead volume as well as the bed voidage. Following integration of the area behind the breakthrough curve, the amount of the enzyme bound was determined by subtraction. The physical characteristics of the feed solutions are summarised in Table 4. Loading undiluted fermented broth (98.2 mPa s, shear rate 0.075 s^{-1}) at a flow-rate of 5.8 ml/min (65.6 cm/h) resulted in the multichanelling of the bed and the bed collapsed close to the settled bed height. Introduction of double diluted feed (42.04 mPa s, shear rate 0.476 s^{-1}) resulted in the channel-

ling of feedstock. This channelling of feedstock would decrease the separation efficiency. Channelling of this double diluted feedstock could not be overcome either by suddenly changing the pulse of flow of feedstock or by reversing the direction of flow, as prescribed by Streamline (Amersham Pharmacia). Similar observations have been reported in the recovery of Annexin V using unclarified *Escherichia coli* homogenate [29] and in the purification of glucose-6-phosphate dehydrogenase from unclarified yeast homogenates [30]. Data from the literature are rare regarding biomass content, viscosity and density of the feedstocks. Barnfield Frej et al. [29] recommended a biomass dry mass of 3.5% and a viscosity of less than 10 mPa s at a shear rate of 1 s^{-1}. It was mentioned that feedstocks with viscosity of 50 mPa s at 1 s^{-1} can be handled. Johansson et al. [31] applied a feedstock with 0.6% dry cell mass without commenting upon the viscosity. However, expansion of the bed was trouble-free when the viscosity was close to 21 mPa s. Sharp breakthrough curves were observed at 5- and 10-fold dilution of the fermented broth (Fig. 5). This may be due to lower viscosity of the diluted feed. Comparing 5-, 10- and 20-fold diluted feed samples, the feed density, cell protein concentration and enzyme activity decreased with increase in dilution, whereas there was no appreciable change in viscosity with dilution (Table 4). The required superficial velocity for 5-, 10- and 20-fold diluted feed samples of the bed increased with the increase in dilution for double expansion of the bed. This is due to a decrease in feed density with increased dilution (Table 4). The V_b, t_b, Q_b, *DAC* and *DAR* of various diluted samples were calculated and are tabulated in Table 5. The breakthrough volume and breakthrough time increased with dilution. The *DAC* and *DAR* values for 5-fold diluted feed sample were the maximum due to the dominance of adsorption kinetics, as is evident from the uptake curve (Table 5). The bed equilibrium capacities of the feed on expanded bed were less than that of the maximum batch equilibrium capacity. This is perhaps due to intraparticle hindrance (at higher viscosity of the feed) on expanded bed, which slowed the adsorption. On the other hand, the higher value obtained for the capacity of the adsorbents in batch adsorption is because the estimation is until equilibrium. Dilution of the fermentation broth decreased the viscosity, decreased the enzyme concentration below the K_d value, and thereby slowed the adsorption rate [32]. The decreased slope of the breakthrough curve at 20-fold dilution is due to the slower adsorption kinetics on the bed [32].

The adsorbed enzyme from 5-fold diluted unclarified fermented broth, eluted with 10 m*M* $CaCl_2$ in 50 m*M* Tris–HCl at 25°C, at a flow-rate of 4.4 ml/min (Fig. 6), yielded 94.7-fold increase in enzyme purification with 37.92% recovery. The purified enzyme from the crude unclarified fermented broth of 380-ml volume, containing 6.81 U/ml α-CGTase, with protein concentration 2.65 mg/ml and specific enzyme activity 2.57 U/mg, was eluted out in 28 ml. The protein concentration was 0.1 mg/ml, and enzyme activity 25.25 U/ml with specific enzyme activity 243.47 U/ml was obtained in the eluted protein.

This purification of α-CGTase obtained on expanded bed was compared to the reported purification of this enzyme by various methods. An UF concentrated α-CGTase was applied to a modified starch column and the enzyme was eluted from the column with 10 m*M* $CaCl_2$ (in 50 m*M* Tris–HCl, pH

Table 5
Comparison of breakthrough points (volume/time) on affinity-HEG beads at various dilutions of fermented broth

H_0 (cm)	Dilution factor	u (cm/h)	V_b (ml)	t_b (min)	*DAC* (U/ml)	*DAR* (U/ml per min)	Q_b (U/ml)
7.5	5	105.0	194.0	20.90	33.86	1.62	46.85
7.5	10	130.0	355.0	30.90	30.46	0.99	39.24
7.5	20	152.0	447.2	33.27	20.78	0.62	36.37

H_0 is the settled bed height and u is the superficial velocity of the feed. V_b and t_b are the breakthrough volume and time of the bed considering effluent enzyme concentration 5% of the feed enzyme activity. *DAC* and *DAR* are the dynamic adsorption capacity and rate of the bed, respectively. Q_b is defined as maximum bed adsorption capacity.

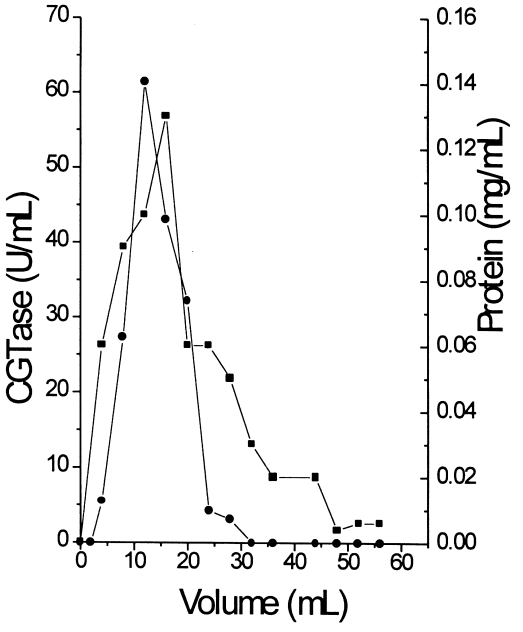

Fig. 6. Elution profile of α-CGTase and protein. ● CGTase activty (U/ml), ■ protein concentration (mg/l).

7.5) at 25°C with 82% recovery [17]. This enhanced recovery of the enzyme was a result of liquifaction of the modified starch (as adsorbent) during the elution and the enzyme came out easily from the pores. Starch, cyclodextrin produced from liquefied starch and $CaCl_2$ provided extra stability to the enzyme. A 29-fold purified enzyme was obtained from the starch column. There are a number of references on CGTase purification, using α-CD as ligand on packed bed. In one report, α-CD was coupled to Sepharose 6B via dioxirane to purify CGTase [33]. This one step procedure with α-CGTase yielded 113-fold purification, with 90–92% recovery. In another work, Sepharose 6FF-α-CD matrix was used to purify α-CGTase directly from cell free culture broth [34]. A 35-fold enzyme purification, with 79% enzyme recovery, was noted. Crude extract was adsorbed on starch, the desorbed enzyme was concentrated by $(NH_4)_2SO_4$ precipitation and finally purified on Sepharose 4B-α-CD [35]. A 59.7-fold purification with 54% recovery of the enzyme was reported by this method. In all these CD affinity based separation of CGTase, the enzyme was eluted with the corresponding cyclodextrin solution and this resulted in increased recovery.

4. Conclusions

The macroporous beaded copolymer of HEMA-EGDM was derivatized by TDI and subsequently coupled to α-CD to obtain affinity-HEG beads. A number of distributor plates, of varying thickness, were fabricated and the hydrodynamics of the affinity-HEG beads were studied in a column containing the distributor plate. A 2-mm thickness distributor plate was found to be the most suitable one. Cyclodextrin glycosyltransferase in fermented broth was selected as model system due to its process complexity in clarification. Feeding 5-fold diluted feed to the EBA column resulted in trouble-free expansion of the bed and in a sharp breakthrough curve. The enzyme CGTase was purified on EBA with 95-fold purification and 38% of the enzyme was recovered. The chromatographic matrices reported in this communication have excellent chemical and mechanical stability and are not affected by the variation in process parameters in purification of CGTase. The matrices are resistant to microbial attack also.

5. Nomenclature

C	Enzyme concentration in the effluent (U/ml)
C_0	Inlet enzyme concentration in the feed (U/ml)
CD	Cyclodextrin
CGTase	Cyclodextrin glycosyltransferase
CLD	Crosslink density
D_{or}	Diameter of the hole
DAC	Dynamic adsorption capacity (U/ml of the adsorbent)
DAR	Dynamic adsorption rate (U/ml of adsorbent/min)
D_{ax}	Axial dispersion coefficient
DEAE	Diethyl amino ethane
DMSO	Dimethyl sulfoxide
EGDM	Ethylene glycol dimethacrylate
H_0	Settled bed height (cm)

H	Expanded bed height (cm)
HEG	Copolymeric macroporous HEMA and EGDM
HEMA	2-Hydroxy ethyl methacrylate
I.D.	Internal diameter (mm)
K_d	Dissociation constant, U/ml
kDa	Kilodalton
m	Units of enzyme applied to the column
N	Number of theoretical plates
Q	Volumetric flow-rate (ml/min)
q^*	Units of enzyme (adsorbate) bound to the adsorbent at equilibrium (U/ml)
Q_b	Maximum bed adsorption capacity
Q_m	Maximum adsorption capacity in batch adsorption (U/g of matrices)
RTD	Residence time distribution
SS	Stainless steel
t_b	Breakthrough time (min)
TDI	2,4-Tolylene diisocyanate
u	Superficial velocity
UF	Ultrafiltration
V	Volume of the feed applied to the column (ml)
V_b	Breakthrough volume (ml)
V_f	Volume of the fluidized or expanded bed (ml)
v_{rf}	Total volume passed through the bed (ml)
ϵ	Bed voidage of expanded bed
ϵ_0	Bed voidage of the packed bed
μ	Viscosity (mPa s)
σ	Dimensionless variance

Acknowledgements

A Senior Research Fellowship awarded to Deba Prasad Nayak from the Council of Scientific and Industrial Research, India, is gratefully acknowledged. The financial support by the Department of Biotechnology, India is also acknowledged. Technical help from Dr Arika Kotha and Dr Omprakash Yemul for matrix synthesis and preparation of affinity matrix is duly acknowledged. Our sincere acknowledgement to Dr Mary McNamara, School of Chemistry, Dublin Institute of Technology, Dublin, Ireland, for various technical discussions on cyclodextrins.

References

[1] J.T. Beck, B. Williamson, B. Tipton, Bioseparation 8 (1999) 201.
[2] R. Callewart, L. De Vuyst, Bioseparation 8 (1999) 159.
[3] R.H. Clemmitt, H.A. Chase, Biotechnol. Bioeng. 67 (2000) 206.
[4] A. Lihme, H. Marie, M. Olander, E. Zafirakos, Methods Biotechnol. 9 (2000) 121.
[5] H.A. Chase, Trends Biotechnol. 12 (1994) 296.
[6] G.R. Gilchrist, M.T. Burns, A. Lyddiatt, Spe. Publ. R. Soc. Chem. 158 (Separation for Biotechnology 3) (1994) 186.
[7] C.M. Griffith, J. Moris, M. Robichaud, M.J. Annen, A.V. McCormick, M.C. Flickinger, J. Chromatogr. A 776 (1997) 179.
[8] A. Pai, S. Gondkar, S. Sundaram, A. Lali, Bioseparation 8 (1999) 131.
[9] J.J. Glajch, J.J. Kirkland, J. Kohler, J. Chromatogr. 384 (1987) 81.
[10] M. Asif, N. Kalogerakis, L.A. Behie, Chem. Eng. Sci. 47 (1992) 4155.
[11] A. Kotha, L. Selvaraj, C.R. Rajan, S. Ponrathnam, K. Kumar, G.R. Ambekar, J.G. Shewale, Appl. Biochem. Biotechnol. 30 (1991) 297.
[12] D.P. Nayak, S. Ponrathnam, C.R. Rajan, A. Patkar, O.S. Yemul, Indian patent filed, 2000.
[13] A. Lejuene, K. Sakaguchi, T. Imanaka, Anal. Biochem. 181 (1989) 6.
[14] E.L. McCaffery, in: Laboratory Preparation For Macromolecular Chemistry, McGraw-Hill, New York, 1970, p. 13.
[15] O.H. Lowry, N.J. Rosenbrough, A.L. Farr, R.J. Randall, J. Biol. Chem. 193 (1951) 265.
[16] B.N. Gawande, A.Y. Patkar, Indian patent application no. 1104/DEL/98.
[17] B.N. Gawande, Ph.D. Thesis, University of Pune, India, 2000.
[18] J.F. Richardson, W.N. Zaki, Trans Inst. Chem. Eng. 32 (1954) 35.
[19] N.M. Draeger, H.A. Chase, Bioseparation 2 (1991) 67.
[20] J. Thommes, A. Bade, M. Halfar, A. Karau, M.R. Kula, J. Chromatogr. A 752 (1996) 111.
[21] O. Levenspiel, Chemical Reaction Engineering, Wiley, New York, 1972.
[22] A.-K. Barnfield Frej, H.J. Johanson, S. Johansson, P. Leijon, Bioprocess Eng. 16 (1997) 57.
[23] A. Lindgren, S. Johanson, L.-E. Nystrom, in: B. Henon (Ed.), BED — The Seventh Bioprocess Engineering Symposium, Vol. 27, American Society of Mechanical Engineers, 1993, p. 27.
[24] A. Karau, C. Benken, J. Thommes, M.-R. Kula, Biotechnol. Bioeng. 55 (1997) 54.
[25] Y.-K. Chang, H.A. Chase, Biotechnol. Bioeng. 49 (1996) 512.
[26] G. Garke, W.-D. Deckwer, F.B. Anspach, J. Chromatogr. B 737 (2000) 25.
[27] N. Kuniho, K. Ryuichio, Biosci. Biotechnol. Biochem. 63 (1999) 2064.

[28] D.P. Nayak, S. Ponrathnam, C.R. Rajan, Bioseparation, (submitted for publication).
[29] A.-K. Barnfield Frej, R. Hjorth, A. Hammarström, Biotechnol. Bioeng. 44 (1994) 922.
[30] Y.-K. Chang, H.A. Chase, Biotechnol. Bioeng. 49 (1996) 204.
[31] H.J. Johansson, C. Jegersten, J. Shiloach, J. Biotechnol. 48 (1996) 9.
[32] H.A. Chase, J. Chromatogr. 297 (1984) 179.
[33] E. Laszlo, B. Banky, G. Seres, J. Szejtli, Starch/Starke 33 (1981) 281.
[34] R.D. Wind, W. Liebel, R.M. Buitelaar, D. Penninga, A. Sprint, L. Dijkhuizen, H. Bahl, Appl. Environ. Microbiol. 61 (1995) 1257.
[35] S.A. Ferrarotti, A.M. Rosso, M.A. Marechal, N. Krymkiewicz, L.R. Marechal, Cell. Mol. Biol. 42 (1996) 653.